

Comparison of Thermal Insulation Performance of Fibrous Materials for the Advanced Space Suit

Heather L. Paul¹

Kenneth R. Diller*

Department of Biomedical Engineering,
The University of Texas at Austin,
Austin, TX 78712

The current multi-layer insulation used in the extravehicular mobility unit (EMU) will not be effective in the atmosphere of Mars due to the presence of interstitial gases. Alternative thermal insulation means have been subjected to preliminary evaluation by NASA to attempt to identify a material that will meet the target conductivity of 0.005 W/m-K. This study analyzes numerically the thermal conductivity performance for three of these candidate insulating fiber materials in terms of various denier (size), interstitial void fractions, interstitial void media, and orientations to the applied temperature gradient to evaluate their applicability for the new Mars suit insulation. The results demonstrate that the best conductive insulation is achieved for a high-void-fraction configuration with a grooved fiber cross section, aerogel void medium, and the fibers oriented normal to the heat flux vector. However, this configuration still exceeds the target thermal conductivity by a factor of 1.5. [DOI: 10.1115/1.1611885]

Introduction

Background. The National Aeronautics and Space Administration (NASA) has made it a priority to plan Mars missions, as well as to research and develop the hardware necessary to support these future endeavors. According to the NASA Mars Reference Mission document [1], launch opportunities for cargo missions to Mars will occur as early as September 2007, and the first crew of six could depart from Earth in mid-November 2009. Each manned mission must support crews on the surface of Mars safely and productively for 500 to 600 days. During this time, crewmembers will be required to complete extravehicular activities (EVAs) to construct and maintain the habitat, and to conduct fieldwork, research, and other types of activities to explore the Martian environment. In order to accomplish these EVA tasks successfully, the EMU, commonly known as the space suit, must provide a safe and comfortable internal working environment for the crewmember.

Current EVA expertise is limited to the environments of the Moon and Low-Earth Orbit. Lunar surface environmental vapor pressure is approximately 10^{-8} Pa (10^{-10} torr) or less. At this pressure, there are only traces of helium, hydrogen, neon, and other gases as a consequence of radioactive decay of lunar material. In the lunar environment, radiation is the most important mechanism impacting the thermal performance of the space suit. The absence of a gaseous atmosphere results in exposure to the entire spectrum of solar radiation. The resulting temperatures reach approximately a maximum of 111°C in direct sunlight and a minimum of -171°C in the lunar night.

The Mars environment presents a new challenge for space suit thermal design. A Mars day has a duration of 24.6 hours, and gravity is about 0.38 times that of Earth. The atmosphere consists of 95% CO₂ with an average surface pressure of 800 Pa (6 torr) [2]. The Mars Candor region, one of the favored initial landing sites, experiences a wide range of temperatures. At a typical hot environment in this region, the ranges of both the suit radiation sink temperature (-9°C to -4°C) and the atmospheric surface temperature (-54°C to 27°C) are nominal and will not impair the

thermal performance of the suit. A problem arises in the cold environment, because the surface and atmospheric sink temperatures (-62°C to -46°C and -84°C to -46°C, respectively) are severe [3]. These environmental conditions must be considered in the design of the Mars suit insulation to ensure a system that adequately minimizes heat loss while providing good suit mobility. The target thermal conductivity to provide adequate insulative properties for the suit is 0.005 W/mK.

Currently, multiple material layers, as shown in Fig. 1, cover the EMU. The inner bladder, which maintains suit pressure, is a polyurethane-coated nylon pressure garment. A Dacron™ restraint liner covers and protects the bladder to absorb suit-loading forces, including the pressure load on the suit. The outermost layers of the suit are known as the thermal micrometeoroid garment (TMG) because they primarily provide thermal and micrometeoroid protection. The inner layer of the TMG is a neoprene coated nylon liner designed for the latter purpose. The insulation consists of five layers of aluminized Mylar reinforced with nylon scrim spacers. The outer layer of the TMG, made of Ortho™ material, provides thermal protection, as well as protection against abrasion and tearing.

The multi-layer insulation (MLI) currently used in the space suit has a low overall thermal conductance due to the combination of low radiation absorptivity, high emissivity on its exterior surface, and low thermal conductance between the aluminized layers. This insulation works very well in hard vacuum and has been very effective for application in the lunar and microgravity environments. However, heat loss through the current insulation is expected to be intolerable at Mars pressures. The presence of interstitial gases compromises the insulating properties of multi-layer materials that were designed for use in a radiation-dominated environment. In this configuration, the gas would introduce significant convection and conduction transport components in the MLI for a Mars environment. For this reason, it is necessary to investigate other types of insulation materials.

Previous Testing. Since 1993, various studies have been conducted at the NASA Johnson Space Center (JSC) to evaluate potential Mars insulation concepts. These studies constitute a primary repository of background information for the present investigation.

Studies on Nomex®, an aramid nonwoven fabric, were run with the objective of evaluating the dependence of the effective thermal conductivity of random-fiber thermal insulation on gas-fill pres-

¹NASA Johnson Space Center, Mail Code EC2, Houston, TX 77058.

*Corresponding address: Department of Biomedical Engineering, The University of Texas at Austin, ENS 612, Austin, TX 78712-1084. e-mail: kdiller@mail.utexas.edu.

Contributed by the Bioengineering Division for publication in the JOURNAL OF BIOMECHANICAL ENGINEERING. Manuscript received by the Bioengineering Division June 28, 2001; revision received April 25, 2003. Associate Editor: E. Scott.

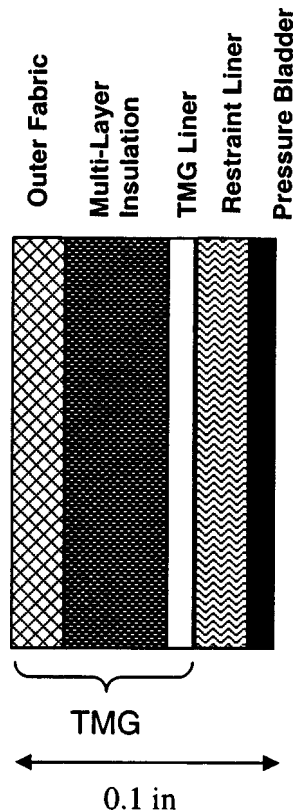


Fig. 1 Layered structure of the current EMU material. The outer layers function as a thermal micrometeoroid garment (TMG).

sure for various gases [4]. Note that the effective thermal conductivity will determine the heat flow through a fabric as a function of the applied temperature differential. It should be primarily a function of the intrinsic conductivity of the solid base material, the properties of the interstitial medium, and the structure of the fibers. Experiments were conducted in vacuum “Chamber V” at JSC using a guarded hot-plate instrument (Holometrix Corporation model TCFGM with Hewlett Packard GP3421A data acquisition system). Tests were conducted in air at 20°C, carbon dioxide at 20°C, 0°C, and -30°C, and nitrogen at -50°C for pressures ranging from vacuum (10^{-4} Pa) to atmospheric (101 kPa). Results showed that the effective thermal conductivity decreased with decreasing gas-fill pressure.

The Phase 1 Mars Candidate TMG Tests were completed in 1994 [5] as the first attempt to evaluate various candidate insulating materials at actual Mars environmental conditions. The thermal performance of four materials were compared to the baseline MLI in the TMG insulation configuration:

- Primaloft, a polyester micro-fiber fill, sandwiched between two layers of nylon rip-stop fabric;
- Polyester waffle weave laminated Mylar with Bostik 5230 web adhesive, aluminized side facing away from the fabric;
- Velcro hook coins (1.5 mm thick, 15 mm diameter) spaced 12 mm apart, attached to the shiny side of Shuttle EMU aluminized mylar using self-sticking adhesive, and sandwiched between two layers of aluminized mylar with the shiny sides facing each other;
- Pink nylon Velcro open weave uncut hooks (3 mm thick) assembled from strips of 55 mm adhesive tape, sandwiched between two layers of Shuttle EMU aluminized mylar with the shiny sides facing each other.

The tests were conducted using the Chamber V guarded hot plate

apparatus with carbon dioxide at pressures from 6 to 250 torr, and temperatures from -30°C to 27°C. The samples were loaded mechanically to 1.0 psi to represent the maximum compression the insulation would experience due to suit pressure and motion. Results showed that the effective thermal conductivity of the TMG lay-ups with fibrous materials at Mars pressure was lower than those with the Shuttle MLI and polyester waffle configurations. Of the fibrous material lay-ups, the Primaloft® configuration had the lowest thermal conductivity (0.017 W/m-K); however this value was still approximately three times greater than the performance goal for Mars applications.

Subsequent Phase 2 tests [5,6] evaluated fibrous insulation samples of Airloft® and Pyroloft® in the TMG configuration at Mars pressure and cold Mars temperatures. As in the Phase 1 tests, candidate insulation materials replaced the MLI of the TMG in the guarded hot plate instrument with argon as the test gas¹. Pressures were from 10^{-5} torr (hard vacuum) to 10 torr (Mars pressure), and temperatures from -100°C to -45°C on the cold side and 20°C on the hot side. Samples were loaded mechanically to 0.1 psi. The Airloft® and Pyroloft® samples demonstrated similar effective thermal conductivities as required for Mars conditions (approximately 0.025 W/m-K).

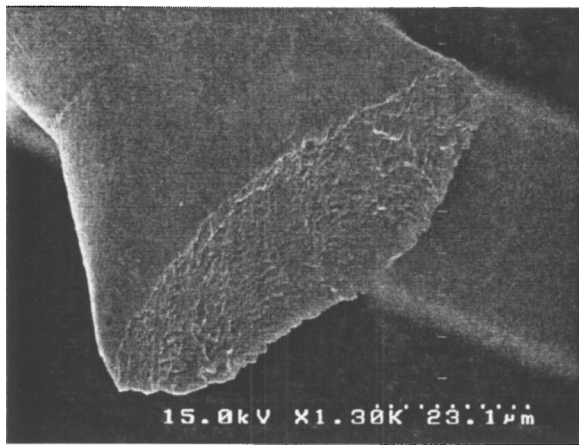
Further studies [7] described thermal performance data for various polyesters and aramids at varying pressures and compressive loads as a function of fiber density, fiber diameter, fabric density, and fabric construction. Primaloft® Sport (Albany International) was chosen for evaluation owing to its high R value and ability to recover from compression. This nonwoven polyester fabric consisted of a 25.4 mm thick blend of 80% fibers of 12 micron or less diameter, 20% fibers of 12 micron or greater diameter, and a low-melt-polyester binder. Fabric density was varied by compression from its original thickness to 16.5 mm, 6.9 mm, or 2.6 mm. Thermal conductivity of all samples increased for greater gas-fill pressure, with the lowest thermal conductivity at high vacuum. At a given pressure, higher density fabric produced lower thermal conductivity, but the performance value at Mars conditions was still significantly higher (0.016 W/m-K) than the benchmark of MLI at vacuum.

Hollofil® (Dupont) fibers were also tested for two different fabric densities (4 and 6 oz/yd²), each needle punched at 120 NPI (needles per inch) or 240 NPI to avoid using bonding materials that could increase the heat transfer [8]. Hollofil® thermal conductivity exhibited a similar dependence on pressure and density, but with values higher than for Primaloft® Sport. None of the samples met the thermal performance goals for conductance of 0.62 W/m²-K and 12.7 mm (0.5 in) insulation thickness.

Various innovative materials have been compared by NASA personnel to identify the most promising candidates for development of the Mars suit insulation [9]. Candidate materials included porous structures [10], active and passive phase change materials, hollow spheres (such as 3M and Zeelan Industries Microspheres and 3M Scotchlite glass bubbles), solvent-gas elements [11], vacuum enclosures [12–15], and fibrous materials [7]. Candidates were ranked in areas of versatility in structure configuration, choice of materials, maturity of industry, insulation experience, flexibility of structure, mechanical strength of structure, continuity of structure, thickness, mass, passive nature and maintainability, robustness, safety and contamination issues, and overall thermal performance. Based on these considerations, fibrous structures were judged to provide the most promise for space suit applications. Thus, they are the subject of the present analysis.

Further thermal conductivity tests were conducted on nonwoven fiber materials at pressures varying from hard vacuum to 8 torr [16]. Three different constructions were evaluated with various fiber deniers, needling intensities, and web densities: solid round fiber (recycled polyethylene terephthalate), hollow fiber

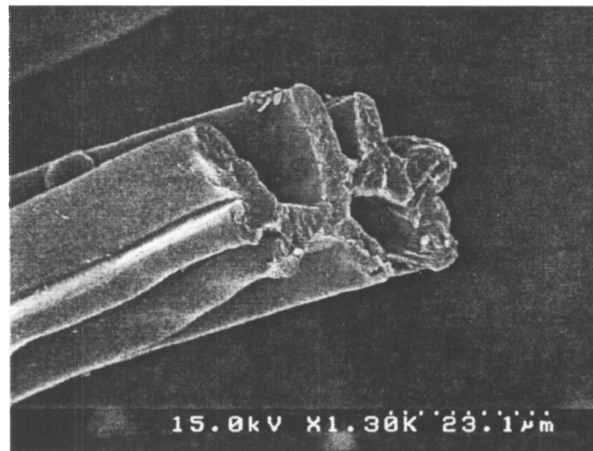
¹The chamber experienced pressure control limitations due to sublimation of carbon dioxide at cold temperatures, so argon was used because its thermal conductivity is close to that of carbon dioxide.



(a)



(b)



(c)

Fig. 2 Scanning electron micrographs of cut fiber cross-sections. (a) solid polyester fiber cross section (25 μm diameter); (b) Dupont Holoofil II[®] fiber cross section ($\sim 25 \mu\text{m}$ outer diameter with four 6 μm holes); (c) 4DG[™] fiber cross section (oblong dimensions: 34 $\mu\text{m} \times 47 \mu\text{m}$).

(Holoofil II[®], Dupont), and multi-lobal fiber (4DG[™] fiber, Eastman Chemical). Scanning electron micrographs are shown in Fig. 2 to illustrate the three relative fiber geometries. All mats were constructed by a process of mechanical entangling of the fibers, known as needle punching, in order to eliminate the effects of thermal, resin, and hydroentanglement bonding. Test configurations embodied two fiber sizes (6 and 15 denier), two needling intensities of 125 and 250 NPI, and web volume densities from 75 to 143 kg/m^3 . The simple calculation for converting fiber size specifications in denier to diameter is presented in Appendix A. The fiber diameters were approximately 25 μm (6 denier) and 40 μm (15 denier). For the range of pressures and temperatures tested, the 4DG[™] fiber material had the best conductive insulation properties. Other parametric results showed that smaller fiber size and higher fiber web density decreased thermal conductivity. This study demonstrated that the fiber insulations could perform almost as well as MLI in high vacuum applications (i.e., in radiation-dominated conditions), plus the fibrous structure could inhibit the formation of internal natural convection loops which would compromise insulation in a gaseous environment.

Methods

The primary objective of the present investigation was to determine the impact of varying fiber cross section, fiber orientation with respect to heat flow, and interstitial material and void fraction on the effective thermal conductivity of fibrous insulations. Numerical simulations were performed for a unit cell system constructed of a single solid or evacuated fiber surrounded by a medium composed of gaseous argon, carbon dioxide or solid aerogel. Details of the model and constitutive property data follow.

Heat Transfer in Fibrous Materials. The overall heat transfer in fibrous matrix materials is the sum of contributions through the fiber and interstitial medium, which may involve multiple transport mechanisms. Conduction occurs in the solid fiber material and the medium trapped in the spaces between the fibers, free convection in the presence of a gravity field if the medium is gaseous and if the space is large enough to support buoyancy driven factors, and radiation with the environment at the surface of the fabric assembly, and internally among the fibers. In order to minimize the effective thermal conductivity of a fibrous material,

it is necessary to find the balance between minimizing fiber content to reduce conduction, while providing enough fibers to prevent convection and to decrease radiation effects. In addition, non-thermal considerations, such as mechanical strength, may dictate important considerations in material design.

In designing an approach to analysis, it is necessary to determine the relative contributions of the various modes of heat transfer through the insulating material. Conduction is understood to be an important component of heat transfer. Whether natural convection should be included is dependent on the comparison of the magnitudes of buoyancy-driven movement of gas phase in void spaces and the viscous retardation of such movement. If the ratio of these effects as expressed in terms of the dimensionless Rayleigh number exceeds a threshold value on the order of 10^3 [17], the natural convective effects will be suppressed, and heat transfer will occur primarily via conduction. The Rayleigh number was calculated for conditions that would lead to the highest possible value in order to determine if there was any possibility that natural convection might play a role in heat transfer through the garment insulation:

$$Ra_L = \frac{g(1/T)(T_H - T_C)L^3}{\alpha\nu}$$

where g is the acceleration of gravity on Mars, L is the enclosed void dimension, α is the thermal diffusivity and ν is the kinematic viscosity. The constitutive properties were evaluated for CO_2 at 260 K, near the top temperature range that would be encountered. The applied temperature differential is also the maximum that would be encountered, 300 K–180 K=120 K. The dimension of the enclosed convective cavity corresponds to the largest void size of about 500 μm . For this set of parameters, the value of the Rayleigh number is about 10^{-1} , which is four orders of magnitude less than the threshold for significant natural convection. Thus, the analysis presented herein assumes that the insulation effectiveness is dictated solely by conductive transport.

Aerogels. Because of advances in the thermal performance of aerogel materials, silica aerogel is being considered as a medium to fill the interstitial space among fibers, thereby mechanically obviating any potential internal convection and radiation. Silica aerogel is a low-density, highly porous material, known for its super-insulating characteristics. As summarized in [18], aerogels are prepared using sol-gel processing techniques followed by extraction of a solvent in a supercritical state. An organic silicon compound, such as tetraethylorthosilicate (TEOS), is mixed with water, alcohol (ethanol), and various catalysts. This mixture is poured into a mold, where hydrolysis occurs between the water and TEOS. The resulting silica ester condenses to form an alcocol, a suspension of silica particles. These particles grow and intertwine, creating a highly porous, semisolid structure called an alcocol. Supercritical extraction of the alcohol filling the void spaces removes the liquid solvent without damaging the microstructure, leaving a low-density solid substance, called aerogel. Aerogels have a very low solid material density (0.02 to 0.4 g/cm^3), and a very high internal surface area (900 to 1000 m^2/g) [18]. Based on the combination of its solid microstructure, low density, and silica composition, aerogels show great promise as an insulation medium. Manufacturer supplied data for the thermal conductivity of aerogel and an aerogel/carbon fiber composite are given as a function of environmental vapor pressure in Fig. 3.

Fiber Types. The three fiber constructions tested in [16] were evaluated numerically in this study: round fibers with a solid cross section, Dupont Holofill II® fibers that are round with four holes along the length of the fiber, and 4DG™ Fit Type 401 fibers from Eastman Chemical, having a cross-section with deep grooves along the longitudinal axis (Fig. 2). Fiber sizes of 6 and 15 denier were evaluated for each fiber type.

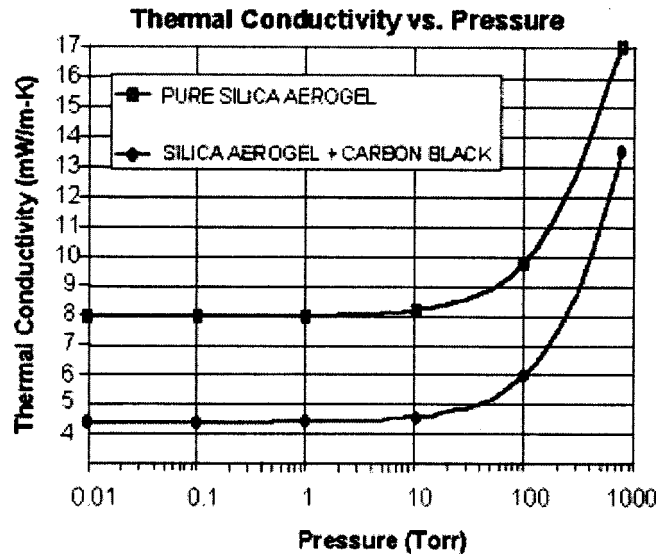


Fig. 3 Thermal conductivity for aerogel and aerogel and an opacifying agent as a function of pressure (manufacturer's data) [18]

Unit Cell Model. A unit cell model consisting of a single fiber surrounded by a concentric rectangular interstitial void was created for each of the three fiber types using SolidWorks™ software. Four cases of steady-state conduction were evaluated to compare the effective thermal conductivity at extreme high (H) and low (L) interstitial void fractions for perpendicular (P) and axial (A) orientations of the fiber to the temperature gradient and were coded according to the defined designating letters.

Void fraction (VF) is defined as the ratio of interstitial void volume to total unit cell volume:

$$VF = \frac{V_{void}}{V_{total}} = \frac{V_{total} - V_{fiber}}{V_{total}} = 1 - \frac{V_{fiber}}{V_{total}}$$

Since the unit lengths of the fiber and void medium are equal, the void fraction can be expressed in terms of the cross-sectional areas as:

$$VF = 1 - \frac{A_{fiber}L}{A_{total}L} = 1 - \frac{A_{fiber}}{A_{total}}$$

For each fiber type, limiting values of the void fractions were determined as a function of geometric properties of possible mating configurations to evaluate extremes in the thermal conductivity. To simulate the variations in void fraction, the fiber dimensions were fixed, and the void dimensions were altered from minimum to maximum values. The unit cell model configuration for each fiber type is depicted in Fig. 4.

Solid Fiber Model Construction. The solid fibers have a uniform, round cross-section of either 25 or 40 micron diameter. For a low void fraction, the dimensions of the unit cell were set 0.1 micron greater than the outer fiber diameter, i.e., 25.1 μm or 40.1 μm square. For a high void fraction, unit cell dimensions were set 10 times greater than the fiber diameter, i.e., 250 μm or 400 μm square. By simple geometric calculations, the interstitial void fractions were approximately $VF_{low} = 27\%$ ($D = 25 \mu m$), $VF_{low} = 25\%$ ($D = 40 \mu m$), and $VF_{high} = 99\%$ ($D = 25 \mu m$ and 40 μm).

Hollow Fiber Model Construction. The hollow fiber cross-sections were built based on the assumption of a circular hole geometry of 9 μm or 6 μm for the large and small fibers, respectively. Other cell dimensions were matched with those of the solid

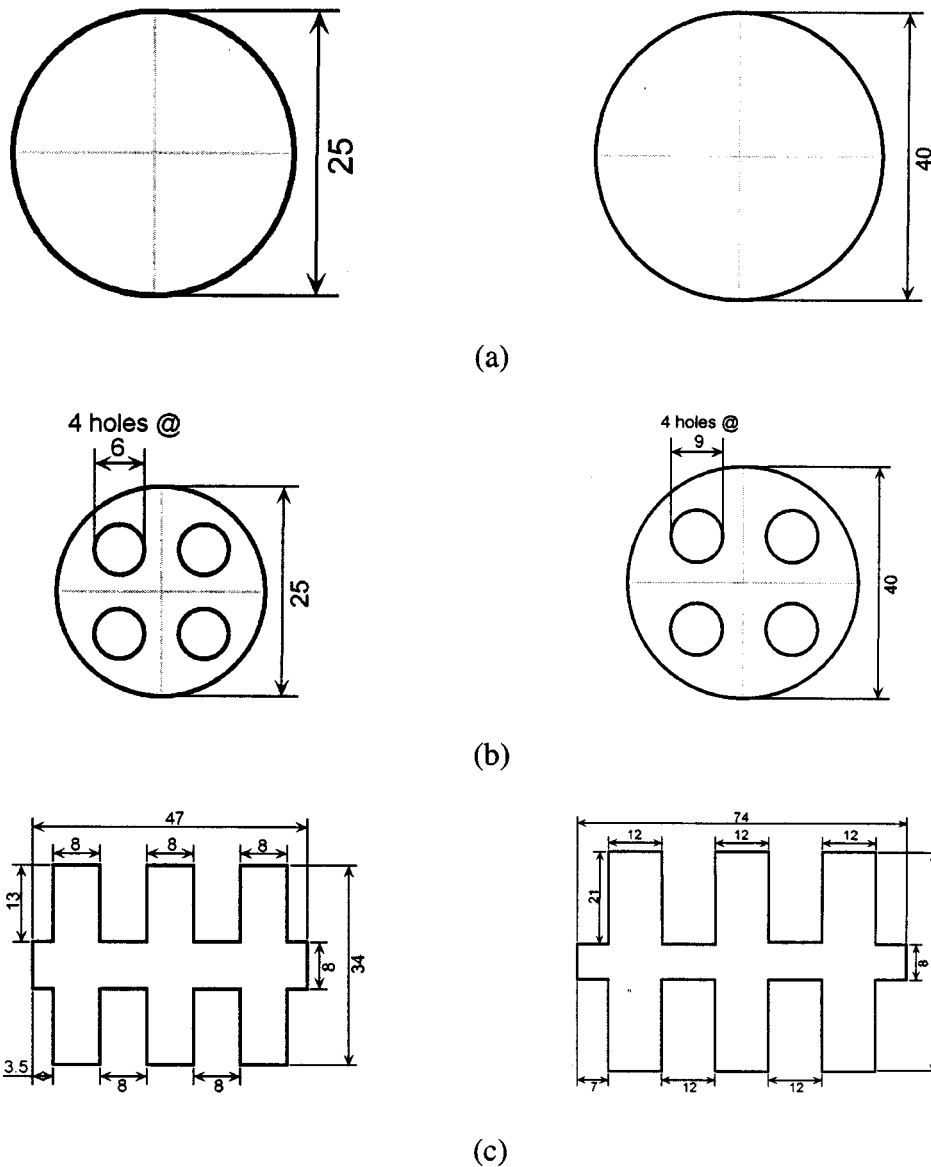


Fig. 4 Model cross-sectional dimensions of the (a) solid, (b) hollow, and (c) 4DG™ fibers (dimensions in microns). 6 denier is on the left and 15 denier on the right.

fibersⁱⁱ for all four cases, yielding void fractions of $VF_{low} = 44\%$ ($D = 25 \mu\text{m}$, $d = 6 \mu\text{m}$), $VF_{low} = 40\%$ ($D = 40 \mu\text{m}$, $d = 9 \mu\text{m}$), and $VF_{high} = 99\%$ ($D = 25 \mu\text{m}$ and $40 \mu\text{m}$).

4DG™ Fiber Model Construction. The 4DG™ fibers have a more complex geometry due to their deep channels along the longitudinal axis. The fiber cross sections were approximated using rectangular lobes with dimensions taken from [19]. To model the low void fraction case, the void cross-section was built 3 micronsⁱⁱⁱ larger than the outer fiber dimensions, i.e., $37 \times 50 \mu\text{m}^2$ and $53 \times 77 \mu\text{m}^2$. For high void fractions, unit cell boundaries were set 10 times greater than the fiber outer dimensions, i.e., $370 \times 500 \mu\text{m}^2$ and $530 \times 770 \mu\text{m}^2$. Simple geometric calculations were used to determine the approximate high and low interstitial

void fraction values for the 4DG™ fibers. For this case, the calculations are shown to document the more complex assumptions involved.

$$A_{fiber} = [(Area)_{body} + 6(Area)_{lobes}]$$

$$A_{fiber}(6 \text{ denier}) = [(47 \mu\text{m} \times 8 \mu\text{m}) + 6(13 \mu\text{m} \times 8 \mu\text{m})] \\ = 1 \times 10^3 \mu\text{m}^2$$

$$A_{fiber}(15 \text{ denier}) = [(74 \mu\text{m} \times 8 \mu\text{m}) + 6(21 \mu\text{m} \times 12 \mu\text{m})] \\ = 2.1 \times 10^3 \mu\text{m}^2$$

$$A_{total \ low}(6 \text{ denier}) = (37 \mu\text{m})(50 \mu\text{m}) \\ = 1.85 \times 10^3 \mu\text{m}^2 \Rightarrow VF_{low}$$

$$= 1 - \frac{A_{fiber}}{A_{total \ low}} \approx 46\%$$

ⁱⁱOuter diameters used in this study were based on standard values of 6 and 15 denier solid fibers, although Hollofil® II fibers are available in 6.5 and 15 denier sizes. For a 20% internal void fraction, this equates to outer diameters of 28.3 and 42.9 microns.

ⁱⁱⁱ3 microns was the smallest dimension that the software would allow for the analysis setup.

$$\begin{aligned}
A_{total\ high}(6\ \text{denier}) &= (370\ \mu\text{m})(500\ \mu\text{m}) \\
&= 1.85 \times 10^5\ \mu\text{m}^2 \Rightarrow VF_{high} \\
&= 1 - \frac{A_{fiber}}{A_{total\ high}} \approx 99\% \\
A_{total\ low}(15\ \text{denier}) &= (53\ \mu\text{m})(77\ \mu\text{m}) \\
&= 4.08 \times 10^3\ \mu\text{m}^2 \Rightarrow VF_{low} \\
&= 1 - \frac{A_{fiber}}{A_{total\ low}} \approx 48\% \\
A_{total\ high}(15\ \text{denier}) &= (530\ \mu\text{m})(770\ \mu\text{m}) \\
&= 4.08 \times 10^5\ \mu\text{m}^2 \Rightarrow VF_{low} \\
&= 1 - \frac{A_{fiber}}{A_{total\ high}} \approx 99\%
\end{aligned}$$

Finite-Element Model. Analysis of heat transfer within the unit cell models was implemented with COSMOS DesignSTAR™ software that incorporates a fast finite-element solver. Boundary conditions were set to match the system parameters used in the JSC-guarded hot-plate experiments [7,16]: a gas pressure of 8 torr and isothermal surfaces imposed on two opposing sides of the unit cell equal to hot and cold plate temperatures of 273 K and 243 K, with all remaining sides insulated.

Three different interstitial void media were evaluated: argon, to match the JSC experiments [16]; carbon dioxide, to represent the atmospheric environment of Mars; and aerogel. For gases, thermal conductivity is a function of temperature, but can be assumed independent of pressure for values down to 1 torr. Gas thermal conductivity values were evaluated at an approximate mean temperature of 260 K [20]. The thermal conductivity of pure silica aerogel decreases with decreasing pressure (Fig. 3) [21]; the value at 8 torr (approximately 0.0082 W/m-K) was used.

For the purpose of this analysis, the thermal conductivities of the three fiber types were assumed to be neither temperature nor pressure dependent. The conductivity for solid round polyester fibers was 0.045 W/m-K [21], nearly 10 times the target value. The thermal conductivity of the hollow and 4DG™ fibers was calculated from clo values given by manufacturers^{iv}. The clo rating for Hollofil II® fibers is 1.5 for a 0.6 in thick sample [22], from which the thermal conductivity was determined by simple algebraic manipulation.

$$\begin{aligned}
R &= \frac{(1.5\ \text{clo}) \left(\frac{0.18\ \text{°C} \cdot \text{m}^2 \cdot \text{hr}}{\text{clo}} \right) \left(\frac{3600\ \text{s}}{\text{h}} \right) \left(\frac{\text{kcal}}{4186.6\ \text{J}} \right) \left(\frac{\text{J/s}}{\text{W}} \right)}{(0.6\ \text{in}) \left(\frac{\text{m}}{39.37\ \text{in}} \right)} \\
&= 15.23\ \frac{\text{°C} \cdot \text{m}}{\text{W}} \\
k &= 1/R = 0.0656\ \frac{\text{W}}{\text{m} \cdot \text{K}}
\end{aligned}$$

For evacuated fibers, a composite thermal conductivity was calculated based on applying the value for solid fiber to the material and setting the value in the holes to approach zero. The thermal conductivity value for the 4DG™ fiber was determined from clo data [23] as 0.01624 W/m-K (details of this calculation are given in Appendix B.)

^{iv}The clo rating of a clothing ensemble is a dimensionless unit used to express the total thermal resistance from the skin to the outer surface of the clothing. One clo is equal to 0.155 (°C-m²)/W.

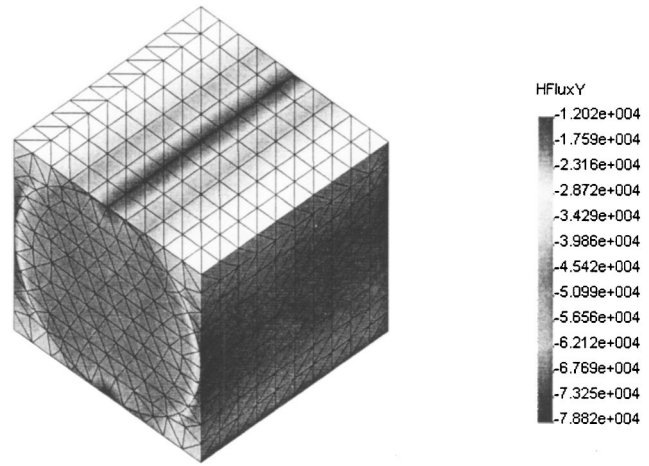


Fig. 5 Surface distribution of heat flux for a simulation of a solid fiber with argon gas interstitium, low void fraction and perpendicular orientation of the fiber with the temperature gradient (heat flux units are W/m²). This subsystem represents the smallest repeated structural unit of the insulation with full material thickness and a single fiber with its surrounding interstitium.

The finite-element solution provided a value for the steady state heat flux for all of the surface nodes on the grid, which were then integrated over the entire surface to obtain the total heat transfer under specific operating conditions. Fig. 5 shows the surface heat flux distribution for LP (low interstitial void fraction, perpendicular orientation to the applied temperature gradient) conditions applied to a solid fiber. The effective thermal conductivity was calculated for the net heat transfer over the entire cross-sectional flow area of the unit cell and the applied temperature gradient.

Results and Discussion

Finite element analysis was performed to evaluate the influence of three fabric materials, two fiber diameters, three interstitial compositions, two extreme orientations to heat flow, and two extreme void fractions on steady state heat transfer through the unit cell suit insulation models.

Figures 6 and 7 present 15 denier fiber data for low and high interstitial void fractions, respectively. High void fraction systems clearly have better insulation performance than do low void fraction, as would be expected since the thermal conductivities of all interstitial media are less than of the fibers. As the fraction of low

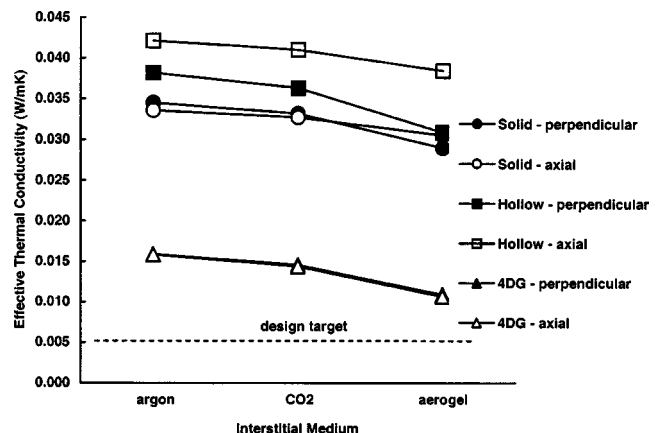


Fig. 6 Effective thermal conductivity of 15 denier fiber insulation materials for low interstitial void fraction as a function of fiber type, interstitial medium and fiber orientation

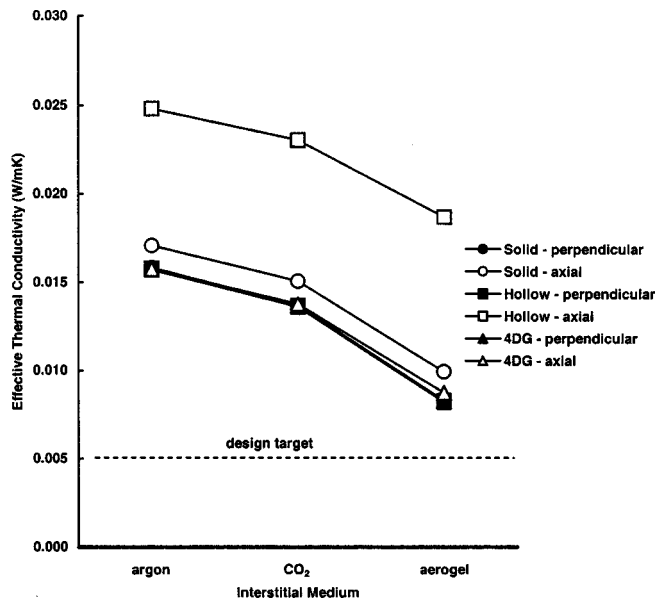


Fig. 7 Effective thermal conductivity of 15 denier fiber insulation materials for high interstitial void fraction as a function of fiber type, interstitial medium and fiber orientation. Note that the data for the perpendicular orientations are so similar that the curves are indistinguishable.

conductivity material in the unit cell increases, so does the insulating capability. At low void fraction, where the fiber occupies a greater portion of the system, the 4DG™ type offers much better insulation. Owing to its geometry, the 4DG™ unit cell is composed of 40% interstitial medium, as opposed to 25% for the solid and hollow fiber types. Since the 4DG™ fibers allow for a greater proportion of low conductivity interstitial medium per unit cell, they also provide more effective overall insulation. As the interstitial void fraction becomes larger, this effect is diminished.

The effect of fiber orientation with respect to the heat flow vector is apparent by comparison of the multiple curves contained within Figs. 6 and 7. As the portion of the unit cell consisting of fiber becomes larger, the influence of the fiber orientation diminishes. The maximum orientation effect is found in the extreme case in which the fiber occupies the minimum possible portion of the unit cell. When the fiber is aligned axially with the heat flow, it provides a relatively high conductivity pathway across the unit cell in parallel with the interstitial medium which is less conductive, thereby compromising the overall insulating capacity. A fiber normal to the heat flow provides no such direct conduction pathway and requires that heat transfer occur primarily through the interstitial void medium. When the void fraction is small, the fiber occupies a much larger fraction of the unit cell volume, and orientation is less significant.

By comparison of the performance of the three different void media, it is clear that the aerogel offers superior insulating properties. The obvious basis for this advantage is the lower thermal conductivity of aerogel than for gaseous argon and CO₂, based on the analysis of heat transport exclusively via conduction.

Table 1 summarizes the overall results for all cases evaluated. The lowest effective thermal conductivity value for the unit cell model is obtained for a 6 denier 4DG™ fiber embedded in an aerogel void medium, with high void fraction and heat flux perpendicular to the fiber (0.00761 W/m-K). Several other systems also approached this level of performance. However, this value is still approximately 1.5 times greater than the target of 0.005 W/m-K required for Mars insulation applications.

An additional computation was performed to evaluate the effect of the material filling the four holes inside the hollow fibers. The holes were modeled as having the conductivity of aerogel or one

Table 1 Computed effective thermal conductivities for all insulating material configurations studied, plus NASA experimental data (n=5) measured for an argon environment. L and H designate low and high interstitial void fractions. P and A designate perpendicular and axial orientation of fibers to temperature gradient. (all values in W/m-K).

Solid—6 denier	Ar	CO ₂	Aerogel
Simulation LP	0.03451	0.03326	0.02912
Simulation LA	0.03342	0.03271	0.03058
Simulation HP	0.01582	0.01371	0.00827
Simulation HA	0.01699	0.01500	0.00982
Experiment (avg/st.dev)	0.02192	±0.00147	
Solid—15 denier			
Simulation LP	0.03447	0.03320	0.02900
Simulation LA	0.03355	0.03273	0.03057
Simulation HP	0.01582	0.01371	0.00832
Simulation HA	0.01707	0.01507	0.00995
Experiment (avg/st.dev)	0.02472	±0.00136	
Hollow—6 denier			
Simulation LP	0.03706	0.03525	0.02981
Simulation LA	0.04315	0.03964	0.03704
Simulation HP	0.01583	0.01372	0.00829
Simulation HA	0.02432	0.02269	0.01832
Hollow—15 denier			
Simulation LP	0.03814	0.03632	0.03088
Simulation LA	0.04210	0.04101	0.03844
Simulation HP	0.01579	0.01369	0.00830
Simulation HA	0.02481	0.02305	0.01870
Experiment (avg/st.dev)	0.0275	±0.00050	
4DG—6 denier			
Simulation LP	0.01477	0.01374	0.01072
Simulation LA	0.01591	0.01463	0.01133
Simulation HP	0.01388	0.01259	0.00761
Simulation HA	0.01575	0.01384	0.00891
Experiment (avg/st.dev)	0.01985	±0.00055	
4DG—15 denier			
Simulation LP	0.01590	0.01460	0.01090
Simulation LA	0.01586	0.01439	0.01065
Simulation HP	0.01570	0.01361	0.00822
Simulation HA	0.01573	0.01378	0.00876
Experiment (avg/st.dev)	0.02343	±0.00265	
Hollow—15 denier (evac)			
Simulation LP	0.03382	0.03267	0.02894
Simulation LA	0.04045	0.03940	0.03764
Simulation HP	0.01578	0.01368	0.00830
Simulation HA	0.02341	0.02190	0.01789

of the two interstitial gases and for comparison, the holes were assumed to be evacuated, with a thermal conductivity of zero. A 15 denier fiber was studied for axial and perpendicular orientations at high and low interstitial void fractions. In all cases, the vacuum insulation gave the best performance, but the differences were small, varying from about 2% (LA) to 6% (HP). It is questionable whether the added costs of producing and maintaining evacuated fibers is worth the added benefit.

Comparison to NASA Experimental Data. One of the goals of this study was to develop a modeling tool to predict the effective thermal conductivity values for a variety of candidate space suit insulation materials. To test the rigor of the model, simulations were conducted that directly matched the conditions under which foregoing NASA experiments were conducted. Table 1 contains NASA experimental data [16] to which the finite elements simulations can be compared. The solid and hollow fiber models are in good agreement with the experiments, but the 4DG™ model data was lower than the NASA values. This difference may be attributed to inaccuracies in derivation of the apparent thermal conductivity for the material from clo data and/or to approximations in the geometric representation of the fiber cross section.

Conclusions

Obtaining the lowest thermal conductivity value required a limiting case 99% void fraction. Under these conditions, the insulation would contain just 1% fiber, which would undoubtedly compromise the structural integrity of any material in a practical space

suit. Extremely large void fraction configurations would be nearly impossible to manufacture and to use. Such configurations could approach the conditions requisite for enabling natural convection heat transfer in the material, but they are impractical for implementation.

This study assumed isotropic conductivity throughout the fiber and that fibers were oriented either perpendicular or axial to the heat flow direction in order to define the extreme performance cases. Future research could study the effects of anisotropic conductivity, and investigate configurations with random fiber orientation.

The thermal conductivity of a pure silica aerogel was used in this study. Further analysis should evaluate aerogels opacified with carbon black or other agents that could lower the effective thermal conductivity of the aerogel materials (Fig. 3). This or similar materials will be necessary to achieve the target thermal insulation performance. Aerogel with embedded carbon fibers would provide improved thermal insulation and also increase the structural integrity of the overall material. Thus, it may be possible to achieve a relatively high interstitial void fraction and still satisfy the thermal and mechanical requirements for the advanced space suit. In addition, the presence of an opacifying agent may have added benefits for thermal radiation insulation, which has been neglected in the present analysis.

This study demonstrated that among the systems evaluated, the 4DG™ fiber and aerogel interstitial void medium provided the best insulation performance. The best configuration consisted of a high interstitial void fraction with heat flux perpendicular to the fibers, although the best performing insulation is still greater by a factor of 1.5 than the target of 0.005 W/m-K for Mars applications. Several other material combinations provided nearly equal performance, so that there is not a single clearly superior choice among the candidate specimens evaluated. Nonetheless, this study sets a direction for future research and testing of fibrous insulation materials. Since it was not possible to meet the design target based on the defined menu of insulating materials, it is recommended that the spectrum of candidates be expanded. Other insulating media options such as encapsulated phase change materials may provide thermal performance sufficient to meet the design criterion.

Acknowledgments

This research was sponsored by a grant from the NASA Johnson Space Center. The authors thank the JSC scientific staff Luis Trevino, Evelyne Orndoff, and Gretchen Thomas for sharing their expertise and advice.

Appendix A-Relationship Between Material Fiber Denier and Diameter

A denier is defined as one gram per 9000 m of fiber linear length, and is a function of the fiber diameter. The following example demonstrates how the diameter of a 6 denier fiber is calculated for the specific gravity of a polyester fiber, 1.34 g/cm³.

$$6 \text{ denier} = 6 \text{ g}/9000 \text{ m}$$

$$V_{\text{fiber}} = \frac{\text{mass}}{\text{Specific Gravity}}$$

$$\left(\frac{\pi}{4} D^2\right) (9000 \text{ m}) = \frac{6 \text{ g}}{\left(1.34 \frac{\text{g}}{\text{cm}^3}\right) \left(\frac{100 \text{ cm}}{\text{m}}\right)^3}$$

$$D \approx 2.5 \times 10^{-5} \text{ m} = 25 \text{ } \mu\text{m}$$

Appendix B: Thermal Conductivity Evaluation of 4DG™ Fiber Batting

Insulation comparison tests were reported for 4DG™ and K431 battings at compression loads up to 1.0 psi [18]. All of this work was presented in USCS units, which are carried forward in this appendix. These data showed that a clo value for an uncompressed 4DG™ sample is approximately 3.75 (hr-ft²-F)/Btu. An apparent thermal conductivity (k_{app}) for the sample can then be determined based on the following relationship:

$$\text{clo} = \frac{\text{thickness}(\Delta x)}{k_{\text{app}}}$$

Unfortunately, no data is available regarding the “natural thickness” of the sample used in this testing, so additional information and assumptions were used to determine the apparent thermal conductivity. Further manufacturer’s data for 4DG™ and round fiber battings show that the thermal conductivity varies slightly from about 0.29 to 0.36 Btu-in/hr-ft²-F over the density range from 0.4 to 1.1 lb/ft³. This data was entered into a spreadsheet and a linear function fit to it to obtain an empirical correlation for this constitutive relationship as:

$$k_{\text{app}}(\text{BTU-in/hr-ft}^2\text{-F}) = -0.0682\rho(\text{lb/ft}^3) + 0.3884$$

Assuming that the samples tested had a constant cross-sectional area (A) throughout the compression testing, the following relationships hold:

$$V = \Delta x \cdot A$$

$$\rho = \frac{m}{V} = \frac{m}{\Delta x \cdot A}$$

The sample tested had a web density of 6 oz/yd², which can be related to the density as:

$$\frac{m}{A} = 6 \frac{\text{oz}}{\text{yd}^2} = 4.167 \times 10^{-2} \frac{\text{lb}}{\text{ft}^2}$$

$$\rho = 4.167 \times 10^{-2} \frac{\text{lb}}{\text{ft}^2} \left(\frac{1}{\Delta x[\text{ft}]}\right)$$

Substituting this result into the correlation equation yields a value for k_{app} , which is then used to determine the clo value:

$$k_{\text{app}} = \frac{\left(-0.0682 \frac{\text{Btu} \cdot \text{in}}{\text{hr} \cdot \text{ft}^2 \cdot \text{F}}\right) \left(4.167 \times 10^{-2} \frac{\text{lb}}{\text{ft}^2}\right)}{\Delta x[\text{ft}]} + 0.3884 \frac{\text{Btu} \cdot \text{in}}{\text{hr} \cdot \text{ft}^2 \cdot \text{F}}$$

$$k_{\text{app}} = \frac{-0.00284}{\Delta x[\text{ft}]} + 0.3884$$

$$\text{clo} \approx 3.75 \frac{\text{hr} \cdot \text{ft}^2 \cdot \text{F}}{\text{Btu}} = \frac{\Delta x[\text{in}]}{k_{\text{app}}} = \frac{\Delta x[\text{in}]}{\frac{-0.00284}{\Delta x[\text{ft}]} + 0.3884}$$

The change in thickness is thus determined to be 1.45 in, and the density is 0.345 lb/ft³. This density value can then be substituted into the correlation equation to predict the apparent thermal conductivity. After conversion to SI units, the apparent thermal conductivity for a 4DG™ fiber batting with a web density of 6 oz/yd² is found to be 0.01624 W/m-K.

References

- [1] Weaver, D. B., and Duke, M. B., 1993, “Mars Exploration Strategies: A Reference Program and Comparison of Alternative Architectures,” AIAA Transactions, **93-4212**, pp. 5–6.
- [2] Essex Corporation, 1989, “Extravehicular Activity in Mars Surface Exploration, Final Report on Advanced Extravehicular Activity Systems Requirements Definition Study,” NAS9-17779, p. 46.

- [3] Iovine, J., and Horton, R., 1999, "Mars EVA Thermal Environment and MPLSS System Analysis Update," NAS9-19100, p. 6.
- [4] Futschik, M. W., 1993, "Analysis of Effective Thermal Conductivity of Fibrous Materials," M.S.E. thesis, University of Houston, Houston, TX.
- [5] Trevino, L. A., and Orndoff, E. S., 1999, "Advanced Suit Insulation Materials Status at Crew and Thermal Systems Division," Internal NASA/JSC Review, Johnson Space Center, Houston, TX, pp. 11–12.
- [6] Cross, C., 1998, "Thermal Conductivity Testing of Several Candidate Insulation Materials for Advanced Space Suit," Advanced Materials Laboratory Quick Look Test Report, AML-98-07, Johnson Space Center, Houston, TX.
- [7] Orndoff, E., and Trevino, L., 2000, "Thermal Insulation Performance of Textile Structures for Spacesuit Application at Martian Pressure and Temperature," *Proc. 2nd International Conference on Safety and Protective Fabrics*, Industrial Fabrics Association, Arlington, VA.
- [8] Verschoor, J. D., Greebler, P., and Manville, N. J., 1952, "Heat Transfer by Gas Conduction and Radiation in Fibrous Insulations," *ASME Transactions*, **74**(6), pp. 961–967.
- [9] Trevino, L. A., and Orndoff, E. S., 2000, "Advanced Space Suit Insulation Feasibility Study," *Proc. 30th International Conference on Environmental Systems*, No. 2001-01-2479.
- [10] Fischer, W. P., Ebeling, W. D., and Haase, B., 1993, "Porous Insulation Performance Under Martian Environment," SAE No. 932116, Warrendale, PA.
- [11] J. P. Stevens and Company, Inc., 1970, "Temperature Adaptable Fabrics," U.S. Patent No. 1,270,216.
- [12] Fisher, A., 1998, "Super Insulator," *Popular Science*, **253**(6), p. 43.
- [13] Winter, J., Zell, M., Hummelsberger, B., Cassese, F., Corsini, R., Wynne, N., Meyer, C., Townsend, P., Nelson, J., and Stifle, K., 1999, "The Refrigerator/Freezer Rack for the International Space Station," SAE J., 1999-01-1943.
- [14] Jones, J., Bard, S., and Blue, G., 1991, "Reversible Chemisorption Gas-Gap Thermal Switch," NASA Tech Brief, **15**(11), Item 59.
- [15] Johnson, D. L., and Wu, J. J., 1997, "Feasibility Demonstration of a Thermal Switch for Dual Temperature IR Focal Plane Cooling," *Cryocoolers 9*, Ross, R. G. ed., Plenum Press, New York, pp. 795–805.
- [16] Tang, H., Orndoff, E., and Trevino, L., 2001, "Thermal Conductivity of Lofty Nonwovens in Space and Planetary Vacuum Environment," 31st International Conference on Environmental Systems, in press.
- [17] Incropera, F. P., and DeWitt, D. P., 1996, *Fundamentals of Heat and Mass Transfer*, 4th Edition, Wiley, New York.
- [18] Hunt, A. J., Jantzen, C. A., and Cao, W., 1991, "Aerogel-A High Performance Insulating Material at 0.1 Bar," *Insulation Materials: Testing and Applications*, II, Graves, R. S. and Wysocki, D. C., eds., American Society for Testing and Materials, Philadelphia, PA, pp. 455–463.
- [19] Fiber Innovation Technology Inc., 2000, "4DG Deep-Grooved Fiber" [Online], p. 6. Available: <http://www.fitfibers.com/publications.htm>
- [20] Hilsenrath, J., Beckett, C. W., Benedict, W. S., Fano, L., Hoge, H. J., Masi, J. F., Nuttall, R. L., Touloukian, Y. S., and Woolley, H. W., 1955, "Tables of Thermal Properties of Gases," National Bureau of Standards, Washington, D.C., pp. 129, 192.
- [21] Gould, G., 2000, "Development of a Suit Insulation Fiber Material for Use in Both Vacuum and Low Pressure Planetary Environments," NAS9-00044, p. 6.
- [22] Benim, T., 2001, personal communication, Dupont Performance Insulations, Kinston, NC.
- [23] Vaughn, E., 2001, Personal communication, Clemson University, Clemson, NC.